

---

---

**Pore size distribution and porosity of  
solid materials by mercury porosimetry  
and gas adsorption —**

**Part 3:  
Analysis of micropores by gas adsorption**

*Distribution des dimensions des pores et porosité des matériaux solides  
par porosimétrie au mercure et par adsorption de gaz —*

*Partie 3: Analyse des micropores par adsorption de gaz*



Reference number  
ISO 15901-3:2007(E)

© ISO 2007

**PDF disclaimer**

This PDF file may contain embedded typefaces. In accordance with Adobe's licensing policy, this file may be printed or viewed but shall not be edited unless the typefaces which are embedded are licensed to and installed on the computer performing the editing. In downloading this file, parties accept therein the responsibility of not infringing Adobe's licensing policy. The ISO Central Secretariat accepts no liability in this area.

Adobe is a trademark of Adobe Systems Incorporated.

Details of the software products used to create this PDF file can be found in the General Info relative to the file; the PDF-creation parameters were optimized for printing. Every care has been taken to ensure that the file is suitable for use by ISO member bodies. In the unlikely event that a problem relating to it is found, please inform the Central Secretariat at the address given below.

.....



**COPYRIGHT PROTECTED DOCUMENT**

© ISO 2007

All rights reserved. Unless otherwise specified, no part of this publication may be reproduced or utilized in any form or by any means, electronic or mechanical, including photocopying and microfilm, without permission in writing from either ISO at the address below or ISO's member body in the country of the requester.

ISO copyright office  
Case postale 56 • CH-1211 Geneva 20  
Tel. + 41 22 749 01 11  
Fax + 41 22 749 09 47  
E-mail [copyright@iso.org](mailto:copyright@iso.org)  
Web [www.iso.org](http://www.iso.org)

Published in Switzerland

# Contents

Page

Foreword.....	iv
Introduction .....	v
1 Scope .....	1
2 Normative references .....	1
3 Terms and definitions.....	1
4 Symbols .....	3
5 Principles.....	5
5.1 General.....	5
5.2 Methods of measurement .....	6
6 Procedure of measurements .....	6
6.1 Sampling.....	6
6.2 Sample pre-treatment .....	6
6.3 Measurement.....	7
7 Verification of apparatus performance.....	7
8 Calibration .....	7
9 Evaluation of the micropore volume.....	7
9.1 General.....	7
9.2 Determination of the micropore volume according to Dubinin and Radushkevich .....	9
9.3 Micropore analysis by comparison of isotherms .....	10
9.4 Determination of micropore size distribution by the Horvath-Kawazoe (HK) and the Saito-Foley (SF) method.....	14
9.5 Determination of micropore size distribution by non-local density functional theory .....	15
10 Test report .....	19
Annex A (informative) Horvath-Kawazoe and Saito-Foley methods.....	20
Annex B (informative) NLDFT method .....	23
Bibliography .....	26

## Foreword

ISO (the International Organization for Standardization) is a worldwide federation of national standards bodies (ISO member bodies). The work of preparing International Standards is normally carried out through ISO technical committees. Each member body interested in a subject for which a technical committee has been established has the right to be represented on that committee. International organizations, governmental and non-governmental, in liaison with ISO, also take part in the work. ISO collaborates closely with the International Electrotechnical Commission (IEC) on all matters of electrotechnical standardization.

International Standards are drafted in accordance with the rules given in the ISO/IEC Directives, Part 2.

The main task of technical committees is to prepare International Standards. Draft International Standards adopted by the technical committees are circulated to the member bodies for voting. Publication as an International Standard requires approval by at least 75 % of the member bodies casting a vote.

Attention is drawn to the possibility that some of the elements of this document may be the subject of patent rights. ISO shall not be held responsible for identifying any or all such patent rights.

ISO 15901-3 was prepared by Technical Committee ISO/TC 24, *Sieves, sieving and other sizing methods*, Subcommittee SC 4, *Sizing by methods other than sieving*.

ISO 15901 consists of the following parts, under the general title *Pore size distribution and porosity of solid materials by mercury porosimetry and gas adsorption*:

- *Part 1: Mercury porosimetry*
- *Part 2: Analysis of mesopores and macropores by gas adsorption*
- *Part 3: Analysis of micropores by gas adsorption*

## Introduction

According to the IUPAC Recommendations, 1984 [42], micropores are defined as pores with internal widths of less than 2 nm. Different methods for the characterization of micropores are available, including spectroscopy, electron and tunnel microscopy and sorption methods. In view of the complexity of most porous solids, it is not surprising that the results obtained are not always in agreement and that no single technique can be relied upon to provide a complete picture of the pore structure. With regard to the application of microporous material as specific sorbents, molecular sieves and carriers for catalysts and biological active material, the field-proven methods of gas sorption are of special value. On account of the fractality of dispersed and porous materials, the results of adsorption measurements depend on the size of the gas molecules used (effective diameter and space required at the surface). Furthermore, micropores might not be accessible for larger molecules and, thus, exclusion effects can be observed.

The measuring techniques of the methods described in the present standard are similar to those of ISO 15901-2 and ISO 9277 for the measurement of gas adsorption at low temperature. From the measured isotherm, however, the very first part (i.e. relative pressures  $< 10^{-1}$ ) is evaluated and thus the evaluation method is different.

© ISO 2007. All rights reserved.

Copyright International Organization for Standardization

# Pore size distribution and porosity of solid materials by mercury porosimetry and gas adsorption —

## Part 3: Analysis of micropores by gas adsorption

### 1 Scope

This part of ISO 15901 describes methods for the evaluation of the volume of micropores (pores of internal width less than 2 nm) and the specific surface area of microporous material by low-temperature adsorption of gases [1],[2],[3],[4],[5],[6],[7]. These are comparative, non-destructive tests. The methods use physisorbing gases that can penetrate into the pores under investigation. The method is applicable to isotherms of type I, II, IV or VI of the IUPAC classification (see ISO 15901-2:—, Figure 1, and ISO 9277).

The methods in this part of ISO 15901 are not applicable when chemisorption or absorption takes place.

### 2 Normative references

The following referenced documents are indispensable for the application of this document. For dated references, only the edition cited applies. For undated references, the latest edition of the referenced document (including any amendments) applies.

ISO 3165, *Sampling of chemical products for industrial use — Safety in sampling*

ISO 8213, *Chemical products for industrial use — Sampling techniques — Solid chemical products in the form of particles varying from powders to coarse lumps*

ISO 9277:1995, *Determination of the specific surface area of solids by gas adsorption using the BET method*

ISO 15901-2:—, *Pore size distribution and porosity of solid materials by mercury porosimetry and gas adsorption — Part 2: Analysis of mesopores and macropores by gas adsorption*

### 3 Terms and definitions

For the purposes of this document, the following terms and definitions apply.

#### 3.1

##### **adsorbate**

adsorbed gas

#### 3.2

##### **adsorption**

enrichment of the adsorptive at the external and accessible internal surfaces of a solid

#### 3.3

##### **adsorptive**

gas or vapour to be adsorbed

- 3.4 adsorbent**  
solid material on which adsorption occurs
- 3.5 adsorption isotherm**  
relationship between the amount of gas adsorbed and the equilibrium pressure of the gas at constant temperature
- 3.6 adsorbed amount**  
number of moles of gas adsorbed at a given pressure,  $p$ , and temperature,  $T$
- 3.7 equilibrium adsorption pressure**  
pressure of the adsorptive in equilibrium with the adsorbate
- 3.8 monolayer amount**  
number of moles of the adsorbate that form a monomolecular layer over the surface of the adsorbent
- 3.9 monolayer capacity**  
volumetric equivalent of monolayer amount expressed as gas at standard conditions of temperature and pressure (STP)
- 3.10 macropore**  
pore with width greater than about 50 nm
- 3.11 mesopore**  
pore with width between approximately 2 nm and 50 nm
- 3.12 micropore**  
pore with width of about 2 nm or less
- 3.13 physisorption**  
weak bonding of the adsorbate, reversible by small changes in pressure or temperature
- 3.14 pore size**  
pore width, i.e. diameter of cylindrical pore or distance between opposite walls of slit
- 3.15 relative pressure**  
ratio of the equilibrium adsorption pressure,  $p$ , to the saturation vapour pressure,  $p_0$ , at analysis temperature
- 3.16 saturation vapour pressure**  
vapour pressure of the bulk liquefied adsorptive at the temperature of adsorption
- 3.17 volume absorbed**  
volumetric equivalent of the amount adsorbed, expressed as gas at standard conditions of temperature and pressure (STP), or expressed as the adsorbed liquid volume of the adsorbate



## 4 Symbols

For the purposes of this document, the following symbols apply, together with their units. All specific dimensions are related to sample mass, in grams.

Symbol	Term	Unit
$K_{Aa}$	Kirkwood-Mueller constant of adsorptive	$J \cdot cm^6$
$K_{As}$	Kirkwood-Mueller constant of adsorbent	$J \cdot cm^6$
$a_s$	specific surface area	$m^2 \cdot g^{-1}$
$a_{s,ref}$	specific surface area of reference sample	$m^2 \cdot g^{-1}$
$\alpha_a$	polarizability of adsorptive	$cm^3$
$a_m$	molecular cross-sectional area	$nm^2$
$\alpha_s$	normalized adsorption (see Note 1)	1
$\alpha_{(s^*)}$	polarizability of adsorbent	$cm^3$
$\beta$	affinity coefficient	1
$c$	speed of light	$m \cdot s^{-1}$
$d_a$	diameter of an adsorptive molecule	nm
$d_{HS}$	diameter of hard spheres	nm
$d_p$	effective pore diameter (cylindrical pore)	nm
$d_s$	diameter of an adsorbent molecule	nm
$d_0$	$d_0 = (d_s + d_a)/2$ , distance between adsorptive and adsorbent molecules	nm
$E$	adsorption potential	$J \cdot mol^{-1}$
$E_0$	characteristic adsorption energy	$J \cdot mol^{-1}$
$\varepsilon_{ff}$	well depth parameter of the gas-gas Lennard Jones potential	K
$\varepsilon_{sf}$	well depth parameter of the gas-solid Lennard Jones potential	K
$k_B$	Boltzmann constant ( $1,380\ 650\ 5 \times 10^{-23}$ )	$J \cdot K^{-1}$
$l$	nuclei-nuclei pore width	nm
$m_a$	mass adsorbed	g
$m_e$	mass of an electron	kg
$m_s$	sample mass	g
$N_A$	Avogadro's constant ( $6,022\ 1415 \times 10^{23}$ )	$mol^{-1}$
$N_a$	number of atoms per unit area (square metre) of monolayer	$m^{-2}$

Symbol	Term	Unit
$N_s$	number of atoms per unit area (square metre) of adsorbent	$m^{-2}$
$n_a$	specific amount adsorbed	$mol \cdot g^{-1}$
$n_m$	monolayer capacity	$cm^3 \cdot g^{-1}$
$p$	pressure of the adsorptive in equilibrium with the adsorbate	Pa
$p_0$	saturation vapour pressure of the adsorptive	Pa
$p/p_0$	relative pressure of the adsorptive	1
$R$	ideal gas constant (8,314 472)	$J \cdot mol^{-1} K^{-1}$
$\rho_g$	gas density	$g \cdot cm^{-3}$
$\rho_{g,STP}$	gas density at STP (273,15 K; 101 325,02 Pa)	$g \cdot cm^{-3}$
$\rho_l$	liquid density	$g \cdot cm^{-3}$
$\sigma$	distance between two molecules at zero interaction energy	nm
$\sigma_{ff}$	distance parameter of the gas-gas Lennard Jones potential	nm
$\sigma_{sf}$	distance parameter of the gas-solid Lennard Jones potential	nm
$T$	temperature	K
$T_{cr}$	critical temperature	K
$t$	statistical layer thickness (see Note 2)	nm
$V_a$	specific adsorbed liquid volume of the adsorbate	$cm^3 \cdot g^{-1}$
$V_g$	specific adsorbed gas volume at STP (273,15 K; 101 325,02 Pa)	$cm^3 \cdot g^{-1}$
$V_{micro}$	micropore volume	$cm^3 \cdot g^{-1}$
$W$	pore width (slit pore)	nm
$\chi_a$	diamagnetic susceptibility of adsorptive	$cm^3$
$\chi_s$	diamagnetic susceptibility of adsorbent	$cm^3$

NOTE 1 According to ISO 31-0 [43], the coherent SI unit for any quantity of dimension one (at present commonly referred to as “dimensionless”) is the unit one, symbol 1.

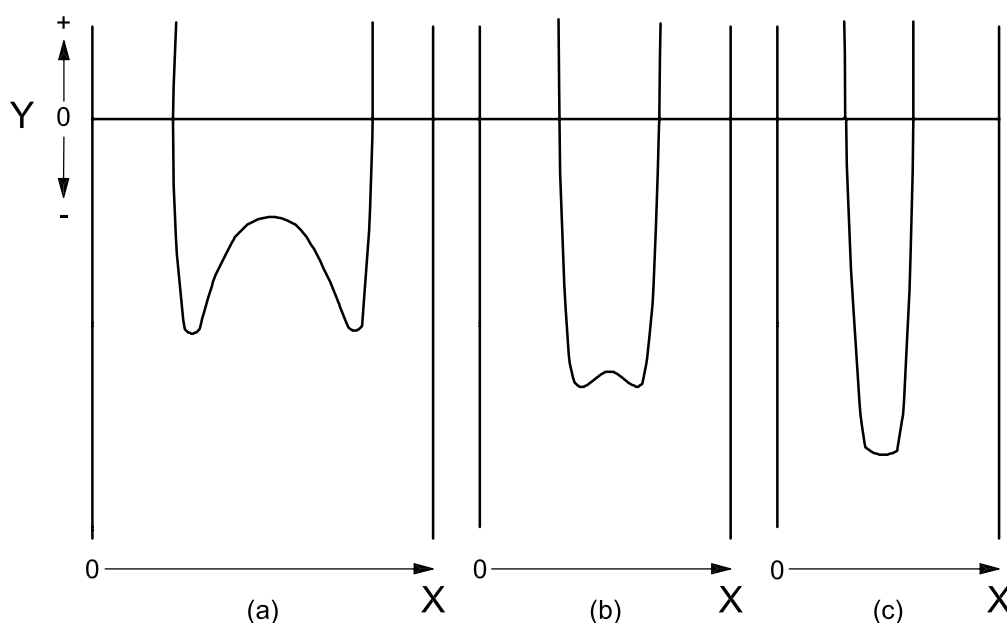
NOTE 2 While the symbol,  $t$ , is generally used to represent time, in the normal practice of pore size distribution analysis by gas adsorption,  $t$  is traditionally used to represent the statistical thickness of the liquid-like adsorbate layer. Therefore, all uses of the symbol  $t$  in this standard will refer to the statistical thickness and not time.

For gravimetric measurements, the mass adsorbed is measured directly (see ISO 9277:1995, Figure 6), but a pressure-dependent buoyancy correction is necessary. Equilibrium is observed by monitoring the mass indication. In the region between about 0,1 Pa to 100 Pa, thermal gas flow can seriously disturb the measurements. Because the sample is not in direct contact with the thermostat, it is necessary to ensure the correct temperature experimentally.

## 5 Principles

### 5.1 General

The methods described in this part of ISO 15901-3 are based on the measurement of the adsorption and desorption of gases at a constant low temperature and the evaluation of the initial part of the isotherm. Gases used are those which are bound by physisorption at the solid surface, in particular  $N_2$  at 77,4 K, Ar at 77,4 K or 87,3 K, and  $CO_2$  at 195 K or 273,15 K. Because of the different size of the gas molecules, and hence, different accessibility of the pores, and also because of the different measuring temperatures, different results can be obtained. In micropores, the potential of interactions of the opposite pore walls are overlapping and, hence, physisorption is stronger than in wide pores or at the external surface<sup>[8]</sup> (see Figure 1). As a consequence, micropores are filled at very low relative pressure ( $< 0,01$ ). A significant portion of the micropores is indicated by a large and steep increase of the isotherm near its origin and subsequent bending to a plateau. Micropores are characterized by the micropore volume and the micropore distribution. Because the pore size is similar to the molecule diameter, the choice of the gas is decisive.



#### Key

- X distance between pore walls
- Y potential energy

**Figure 1 — Three examples of the enhancement of interaction potential between a fluid and the surface in infinitely long, slit-like micropores as a function of the pore width (after Everett and Powl<sup>[8]</sup>)**

The pore size and volume analysis of microporous materials, such as zeolites, carbon molecular sieves, etc., is difficult, because the filling of pores of dimension 0,5 nm to 1 nm occurs at relative pressures of  $10^{-7}$  to  $10^{-5}$  where the rate of diffusion and adsorption equilibration is very slow. Argon at 87,3 K fills micropores of dimension 0,5 nm to 1 nm at appreciably higher relative pressures compared to nitrogen (at 77,4 K). Both the higher pore-filling pressure and higher temperature help to accelerate diffusion and equilibration processes compared to nitrogen adsorption. Hence, it is of advantage to analyse microporous materials by using argon as the adsorptive at liquid-argon temperature (87,3 K). However, as in the case of nitrogen adsorption at 77,4 K, the absolute pressures required to fill the most narrow micropores with argon are still very low. Associated with the low pressures required, is (as indicated above) the well known problem of diffusion restrictions, which prevent nitrogen molecules and also argon molecules from entering the narrowest micropores (as present in activated-carbon fibres, carbon molecular sieves, etc.). This can lead to erroneous adsorption isotherms, underestimated pore volumes, etc. A possibility to overcome these problems (at least for microporous carbons) is the use of  $CO_2$  as the adsorptive at 273,15 K. The saturation pressure at this

temperature is about 3,48 MPa, i.e. in order to achieve the small relative pressures required to monitor the micropore filling, a turbomolecular pump-level vacuum is not necessary. With CO<sub>2</sub> adsorption up to 101 325 Pa (1 atm), one can detect pores from the narrowest micropores up to about 1,5 nm. At these relatively high temperatures and pressures, significant diffusion limitations no longer exist, which leads to the situation that equilibrium is achieved much faster relative to low-temperature nitrogen and argon experiments.

## 5.2 Methods of measurement

The experimental data required to establish an adsorption/desorption (sorption) isotherm may be obtained by volumetric (manometric) or gravimetric methods, by measurements either at stepwise, varied pressure with observation of the equilibrium value of pressure or mass, respectively, or at a continuously varied pressure. Because adsorption/desorption equilibrium can take a long time, the stepwise static method is recommended to ensure the measurement of equilibrium values.

The volumetric method is based on calibrated volumes and pressure measurements (see ISO 9277:1995, Figure 5). The amount of adsorbate is calculated as the difference between the gas admitted and the quantity of gas filling the dead volume (free space in the sample container including connections) by application of the general gas equation. Equilibrium is observed by monitoring the pressure in the free space. It is necessary to take special care in the pressure measurements for micropores as physical adsorption occurs at relative pressures substantially lower than in the case of sorption phenomena in mesopores and can span a broad spectrum of pressures (up to seven orders of magnitude in pressure). Consequently, more than one pressure transducer is necessary to measure the equilibrium pressure with sufficient accuracy. In order to study the adsorption of gases like nitrogen and argon (at their boiling temperatures) within a relative pressure range of  $10^{-7} \leq p/p_0 \leq 1$  with sufficiently high accuracy, it is desirable to use a combination of different transducers with maximum ranges of 0,133 kPa (1 Torr<sup>1</sup>), 1,33 kPa (10 Torr) and 133 kPa (1 000 Torr). In addition, one has to assure that the sample cell and the manifold can be evacuated to pressures as low as possible, which requires a proper high-vacuum pumping system. The desired low pressure can be achieved by using a turbomolecular pump. For gas pressures below about 13 Pa (i.e.  $p/p_0 < 10^{-5}$  for nitrogen and argon adsorption at 77 K and 87 K, respectively), it is necessary to take into account the pressure differences along the capillary of the sample bulb on account of the Knudsen effect (i.e. the thermal transpiration correction).

For gravimetric measurements, the mass adsorbed is measured directly (see ISO 9277:1995, Figure 6), but a pressure-dependent buoyancy correction is necessary. Equilibrium is observed by monitoring the mass indication. In the region between about 0,1 Pa and 100 Pa, thermal gas flow can seriously disturb the measurements. Because the sample is not in direct contact with the thermostat, it is necessary to ensure the correct temperature experimentally.

## 6 Procedure of measurements

### 6.1 Sampling

Sampling shall be performed in accordance with ISO 3165 and ISO 8213. The sample for test shall be representative of the bulk material and should be of an appropriate quantity. Repeated measurements using a second sample are recommended.

### 6.2 Sample pretreatment

The sample should be degassed in vacuum better than 1 Pa at elevated temperature to remove physisorbed material. During this process, irreversible changes of the surface structure (revealed, for example, by a colour change) should be avoided. The highest temperature that can be applied is favourably determined by means of thermogravimetry (see ISO 9277:1995, Figure 3). Otherwise, repeated measurements should be carried out by varying the time and the temperature (see ISO 9277:1995, Figure 4). Also, the temperatures at which materials are evolved from the sample can be determined by means of differential scanning calorimetry and the gas can be analysed.

---

1) Torr is a deprecated unit.

Alternatively, the sample is degassed at an elevated temperature by flushing with a high-quality inert gas, e.g. helium or nitrogen. Complete degassing is indicated by a constant mass or constant pressure, respectively, for a period of 15 min to 30 min. The mass of the dry sample should be determined.

### 6.3 Measurement

Adsorption measurements shall be carried out as described in ISO 9277 or ISO 15901-2.

## 7 Verification of apparatus performance

It is recommended that a certified reference material or a local reference material, selected by the user, be tested on a regular basis to monitor instrument calibration and performance. The local reference material shall be traceable to a certified reference material. Certified reference materials are offered by a number of national standards bodies and are currently available from BAM <sup>2)</sup>, in Germany, and NIST <sup>3)</sup>, in the USA.

## 8 Calibration

The calibration of individual components should be carried out according to the manufacturer's recommendations. Typically, calibration of pressure transducers and temperature sensors is accomplished with reference to standard pressure- and temperature-measuring devices that have calibrations traceable to national standards. Manifold-volume calibration is achieved through appropriate pressure and temperature measurements, using constant-temperature volumetric spaces or solids of known, traceable volume. Analysis tube calibration is generally accomplished through determination of free space described in ISO 15901-2:—, 9.3.

## 9 Evaluation of the micropore volume

### 9.1 General

The isotherm  $V_g = f(p/p_0)$  or  $m_a = f(p/p_0)_T$  can be plotted on a linear scale (see Figure 2) or, preferably, on a logarithmic scale (see Figure 3) of relative pressure.

---

2) Bundesanstalt für Materialforschung und -prüfung (BAM)  
Division I. 1 Inorganic Chemical Analysis; Reference Materials  
Branch Adlershof, Richard-Willstätter-Straße 11, D-12489 Berlin, Germany

3) Standard Reference Materials Program  
National Institute of Standards and Technology (NIST)  
100 Bureau Drive, Stop 2322  
Gaithersburg, MD 20899-2322, USA

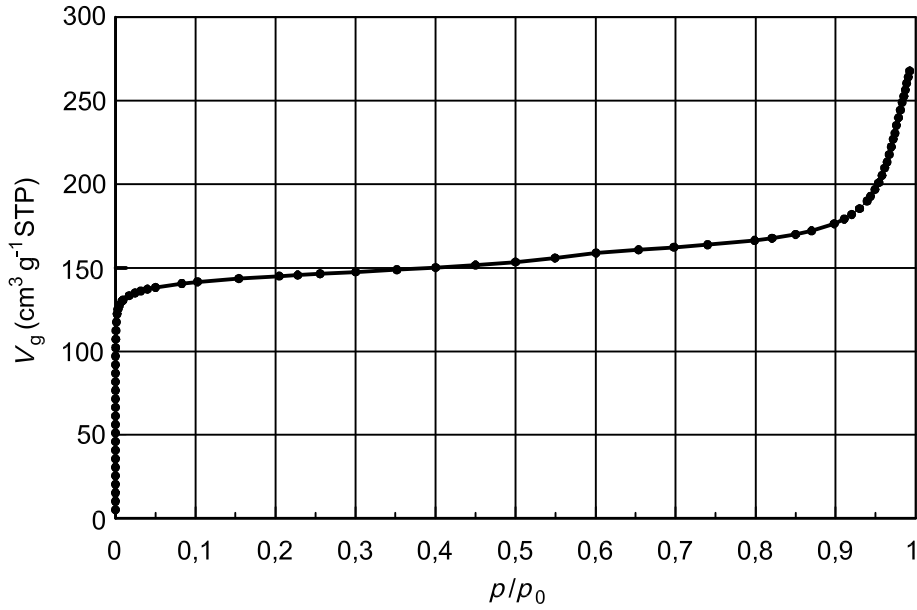


Figure 2 — Linear plot of the isotherm of argon on zeolite at 87,3 K

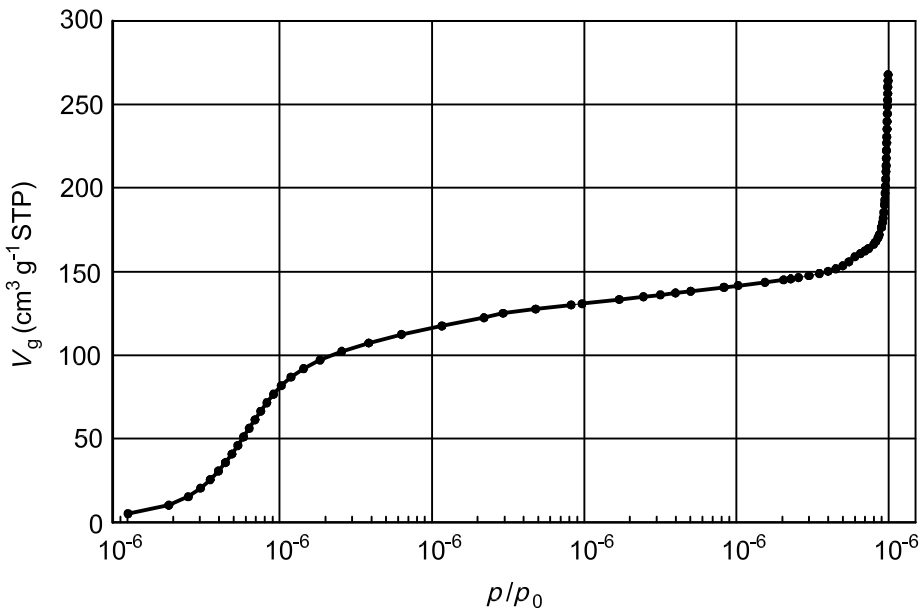


Figure 3 — Semi-logarithmic plot of the isotherm of argon on zeolite at 87,3 K

Adsorption measurements of highly microporous materials result in a Langmuir-type isotherm (type I of the IUPAC classification; see ISO 9277:1995, Figure 1) if the external surface and the volume of mesopores are negligible. The plateau corresponds to the micropore volume. If macropores are present, a steep increase near  $p/p_0 \cong 1$  can be observed.

The amount adsorbed at the plateau is a measure of the adsorption capacity. To obtain the pore volume, it is assumed that the adsorbate has the normal molar volume of the liquid at the operational temperature (liquid density). The pore volume is then given by Equation (1):

$$V_a = m_a / (\rho_l \cdot m_s) \tag{1}$$

## 9.2 Determination of the micropore volume according to Dubinin and Radushkevich

The method, originally developed to investigate the microporosity of activated carbons [9], can be used for any microporous material [10], [11], [12], [13]. The isotherms of the adsorption of pure gases on microporous sorbents can be described by means of Polanyi's potential theory [14]. Each adsorptive/adsorbent system is characterized by an adsorption potential,  $E$ , which is influenced by the particular chemical properties of the adsorbent. The volume,  $V_a$ , filled at a given relative pressure,  $p/p_0$ , as a fraction of the total micropore volume,  $V_{\text{micro}}$ , is a function of the adsorption potential,  $E$ , as given in Equation (2):

$$V_a = f(E) \quad (2)$$

According to Dubinin, the adsorption potential equals the work required to bring an adsorbed molecule into the gas phase. Using Polanyi's potential yields at  $T < T_{\text{cr}}$ ,  $E$  can be defined as given in Equation (3):

$$E = RT \ln \frac{p_0}{p} \quad (3)$$

Based on the Polanyi concept of a temperature-invariant "characteristic curve" (i.e. plots of  $V_a$  versus  $E$ ) for a given adsorbent, Dubinin and Radushkevich arrived at the empirical equation given as Equation (4):

$$V_a = V_{\text{micro}} \exp \left\{ - \left[ \left( \frac{RT}{\beta E_0} \right) \ln \frac{p_0}{p} \right]^2 \right\} \quad (4)$$

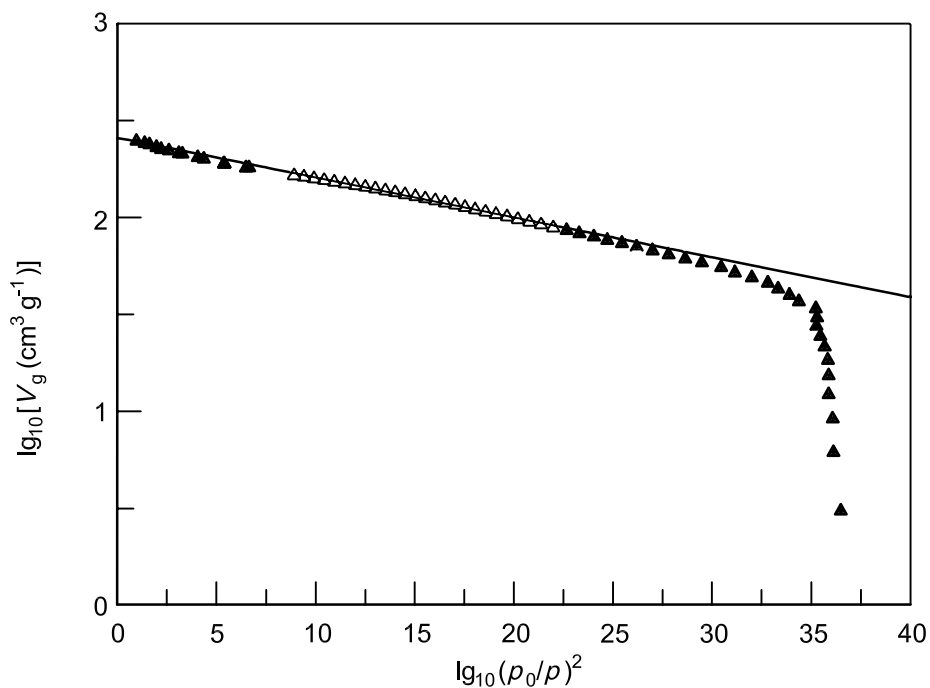
The characteristic adsorption energy,  $E_0$ , is correlated with the pore size distribution. The affinity coefficient,  $\beta$ , allows the scaling of the characteristic curves of different adsorptives (for a given adsorbent) to the characteristic curve of some particular adsorbate, which has been taken as an arbitrary standard. The Dubinin isotherm can now be written in logarithmic form to yield a straight line, as given in Equation (5):

$$\lg V_a = \lg V_{\text{micro}} - D \left( \lg \frac{p_0}{p} \right)^2 \quad (5)$$

where

$$D = 2,303 \left( \frac{RT}{\beta E_0} \right)^2 \quad (6)$$

Data for evaluation should be taken preferably from the region of relative pressure  $10^{-4} < p/p_0 < 0,1$ . Then plot the data on a  $\lg V_g$  versus  $\left[ \lg \frac{p_0}{p} \right]^2$  diagram; see Figure 4. The slope of the regression line gives the parameter  $D$ . The total micropore volume,  $V_{\text{micro}}$ , can be calculated from the ordinate intercept.



**Key**

- ▲ experimental data point
- △ experimental data point used for the Dubinin-Radushkevitch (DR) fit
- DR fit line

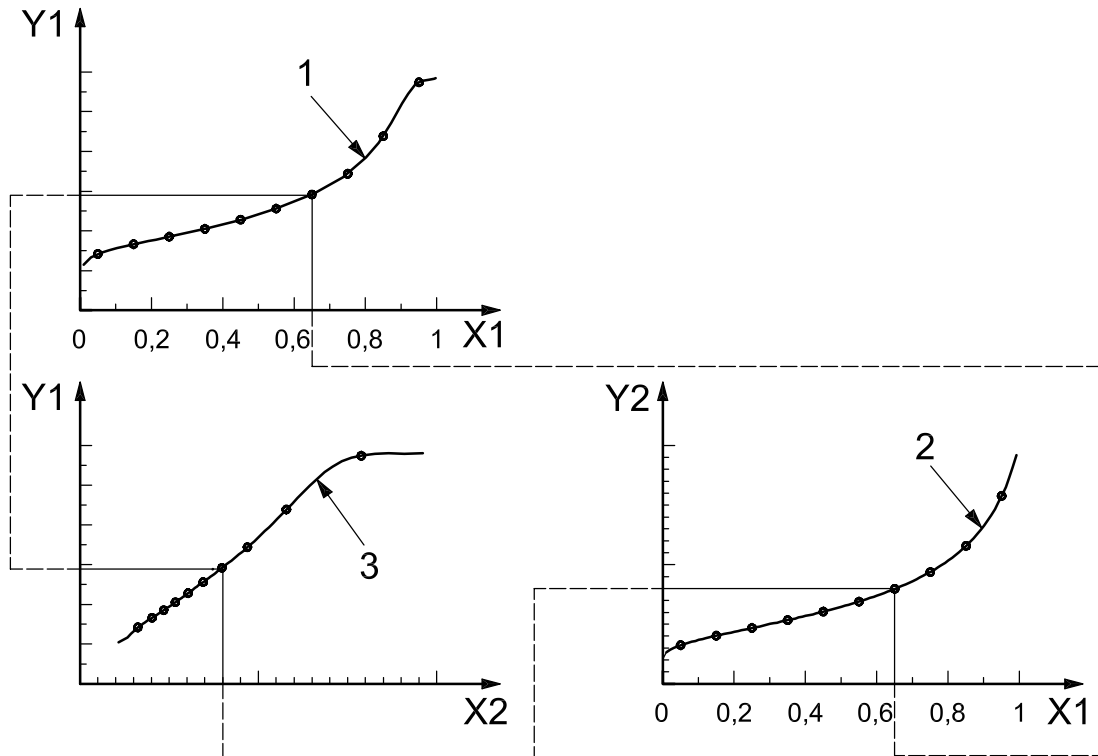
**Figure 4 — Dubinin-Radushkevitch plot of an adsorption isotherm of N<sub>2</sub> at 77,4 K on activated carbon**

### 9.3 Micropore analysis by comparison of isotherms

#### 9.3.1 General

In this method of analysis, gas adsorption isotherms on a sample are compared with those on a non-porous reference material of similar chemical surface composition. The procedure is depicted in Figure 5.



**Key**X1  $p/p_0$ X2  $t$  or  $\alpha_s$ Y1  $V_a$  or  $n_a$ Y2  $t$  or  $\alpha_s$ 

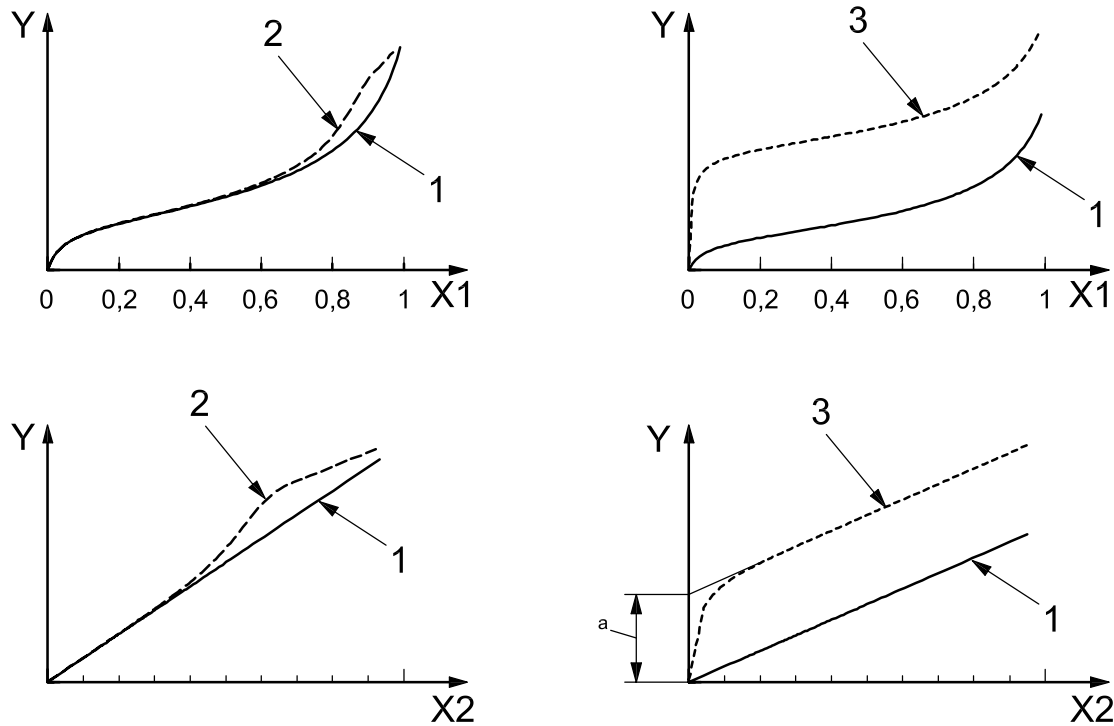
1 sample isotherm

2 reference isotherm

3 resulting comparison diagram

**Figure 5 — Schematic representation of the design of a comparison diagram**

In a comparison plot diagram, the sorption isotherm under test is redrawn as a  $t$ -plot or  $\alpha_s$  plot, i.e. the change of the adsorbed amount is plotted against  $t$  or  $\alpha_s$  values instead of  $p/p_0$ . Characteristic comparison plots are depicted in Figure 6.



**Key**

X1  $p/p_0$

X2  $t$  or  $\alpha_s$

Y  $V_a$  or  $n_a$

1 non-porous material

2 mesoporous material

3 microporous material

a Extrapolated ordinate intercept for  $V_{micro}$ .

**Figure 6 — Isotherms (top) and comparison diagrams (bottom) for three types of materials**

Preconditions for a consistent interpretation of a comparison diagram are the following:

- a) a smooth sample surface in the mesopore region;
- b) micropore filling and capillary condensation occurring in well separated pressure ranges;
- c) multilayer adsorption results in a straight line in the comparison diagram. However, pores cause an upward deviation, permitting an assessment of the pore volume that can be assigned to a certain region of pore width. Within the linear region, the specific surface area,  $a_s$ , of the not-yet-filled pores may be calculated from the slope,  $b$ , as given in Equation (7)

$$a_s = b \frac{a_{s,ref}}{b_{ref}} \tag{7}$$

where

$a_{s,ref}$  is the specific surface area of the reference material;

$b_{ref}$  is the slope of the reference material.

The ordinate intercept corresponds to the volume of pores filled in the respective region at this relative pressure. It can be calculated using Equation (1).

A high proportion of micropores causes a steep increase in the initial part of the curve followed by a linear part. For exclusively microporous materials, the slope of the linear part corresponds to the external surface; when mesopores/macropores are present, it includes the external surface plus that of the mesopore/macropore walls. The extrapolated ordinate intercept of the linear part gives the micropore volume,  $V_{\text{micro}}$ , to be calculated by means of Equation (1). If there are no micropores, the initial part is linear and the specific surface area equals that calculated by the method of Brunauer, Emmett and Teller; see ISO 9277.

### 9.3.2 $t$ -plot method

With the  $t$ -plot method according to Lippens and deBoer [15], [16], [17], [18], the adsorbed amount is designated as a function of the statistical layer thickness,  $t$ , calculated from a standard isotherm of a non-porous sample, as given in Equation (8):

$$t = \frac{V_a}{a_s} = \frac{n_a}{n_m} \sigma_t \quad (8)$$

where  $\sigma_t$  represents the thickness of a single molecular layer, usually taken as 0,354 nm for nitrogen. The specific surface,  $a_s$ , or the monolayer capacity,  $n_m$ , of the reference sample may be determined according to ISO 9277. Equation (8) can be applied for any combination of adsorptive/adsorbent. It allows for the choice of a reference material with a surface of similar chemical composition. With nitrogen at 77 K and using a molecular cross-sectional area  $a_m = 0,162 \text{ nm}^2$  and assuming a tight hexagonal packing of the liquid adsorbate with density  $0,807 \text{ g} \cdot \text{cm}^3$ , Equation (8) takes on the form of Equation (9):

$$t = 0,354 \frac{V_a}{V_m} = 0,354 \frac{n_a}{n_m} \quad (9)$$

In this case, the layer thickness,  $t$ , which represents an average thickness, may be taken from a universal  $t$ -curve as published in the literature (see bibliography) and used in ISO 15901-2.

From the slope of the line depicted in the  $t$ -diagram, the specific surface area can be calculated using Equation (9). If the adsorbed volume is given in cubic centimetres per gram at STP state and the layer thickness,  $t$ , in nanometres, and the slope,  $dV_g/dt$ , has the dimension of cubic centimetres per gram-nanometre, then the specific surface area,  $a_s$ , expressed in square metres per gram, is given by Equation (10):

$$a_s = 1,546 \text{ 8} \frac{dV_g}{dt} \quad (10)$$

The micropore volume,  $V_{\text{micro}}$ , can be determined from the ordinate intercept, as given in Equation (11):

$$V_{\text{micro}} = 0,001 \text{ 546 8} V_g \quad (11)$$

NOTE In the above expression, it is assumed that the density of nitrogen in the micropores is equal to the density of liquid nitrogen. The factor 0,001 546 8 converts the nitrogen volume at STP into the corresponding liquid volume.  $V_{\text{micro}}$  can be considered as an "effective" micropore volume, which acknowledges that this is an oversimplification, as the density of nitrogen in micropores might not be equal to the liquid density.

### 9.3.3 $\alpha_s$ method

This method is not based on a calculation of the layer thickness. Instead, the adsorption for the reference sample is related to a selected relative pressure. In general,  $p/p_0 = 0,4$  is used because at this relative pressure (for nitrogen at 77 K) the monolayer is complete but capillary condensation has not yet started for most materials (with exception of adsorbents which possess mesopores with pore diameters in the range between 2 nm and 5 nm). The reference value,  $\alpha_s$ , is calculated using the reference isotherm as given in Equation (12):

$$\alpha_s = \frac{V_a}{V_a(0,4)} = \frac{n_a}{n_a(0,4)} \quad (12)$$

In the  $\alpha_s$ -diagram, the measured adsorbed amount is depicted as a function of  $\alpha_s$ . The  $\alpha_s$ -diagram looks like the  $t$ -diagram and may be evaluated for the calculation of the specific surface area and the micropore volume in the same manner.

#### 9.4 Determination of micropore size distribution by the Horvath-Kawazoe (HK) and the Saito-Foley (SF) method

Horvath and Kawazoe (HK) [19], [20] describe a semi-empirical, analytical method for the calculation of effective pore size distributions from nitrogen adsorption isotherms in microporous materials. The original HK approach is based on the work of Everett and Powl [8] and considers a fluid (nitrogen) confined to a slit-pore, such as can be found in some carbon molecular sieves and active carbons. Everett and Powl calculated the potential-energy profiles for noble gas atoms adsorbed in a slit between two graphitized carbon layer planes. The separation between nuclei of the two layers is  $l$ . The adsorbed fluid is considered as a bulk fluid influenced by a mean potential field, which is characteristic of the adsorbent-adsorbate interactions. The term “mean field” indicates that the potential interactions between an adsorbate molecule and the adsorbent, which can exhibit a strong spatial dependence, are replaced by an average, uniform potential field. Horvath and Kawazoe found, by using thermodynamic arguments, that by setting the (effective) pore diameter,  $d_p$ , equal to  $l - d_s$ , where  $d_s$  is the diameter of an adsorbent molecule, this average potential can be related to the free-energy change of adsorption, yielding the relationship between the filling pressure,  $p/p_0$ , and the effective pore width, as given in Equation (13):

$$\ln\left(\frac{p}{p_0}\right) = \frac{N_A}{RT} \frac{(N_s K_{As} + N_a K_{Aa})}{\sigma^4 (l - 2d_0)} f_{HK}(\sigma, l, d_0) \quad (13)$$

where

$$f_{HK}(\sigma, l, d_0) = \frac{\sigma^4}{3(l - d_0)^3} - \frac{\sigma^{10}}{9(l - d_0)^9} - \frac{\sigma^4}{3(d_0)^3} + \frac{\sigma^{10}}{9(d_0)^9} \quad (14)$$

The parameters  $d_0$ ,  $\sigma$ ,  $K_{As}$  and  $K_{Aa}$  can be calculated using Equations (15) to (18):

$$d_0 = \frac{d_a + d_s}{2} \quad (15)$$

$$\sigma = \left(\frac{2}{5}\right)^{\frac{1}{6}} d_0 \quad (16)$$

$$K_{As} = \frac{6m_e c^2 \alpha_{(s^*)} \alpha_a}{\frac{\alpha_{(s^*)}}{\chi_s} + \frac{\alpha_a}{\chi_a}} \quad (17)$$

$$K_{Aa} = \frac{3}{2} m_e c^2 a_a \chi_a \quad (18)$$

Equation (13) indicates that the filling of micropores of a given size and shape takes place at a characteristic relative pressure. This characteristic pressure is directly related to the adsorbent-adsorbate interaction energy.

Saito and Foley extended the HK method to the calculation of effective pore size distributions for argon adsorption isotherms at 87 K in zeolites [21], [22]. The basis of the method by Saito and Foley (SF) is again the Everett and Powl potential equation [8], but now only for a cylindrical pore geometry. Following the logic of the HK derivation, Saito and Foley derived an equation, similar to the HK equation, that relates the micropore filling pressure,  $p/p_0$ , to the (effective) pore diameter  $d_p$ :

$$\ln\left(\frac{p}{p_0}\right) = \frac{3}{4} \frac{\pi N_A}{RT} \frac{(N_s K_{As} + N_a K_{Aa})}{d_0^4} f_{SF}(\alpha, \beta, l, d_0) \quad (19)$$

where

$$f_{\text{SF}}(\alpha, \beta, l, d_0) = \sum_{k=0}^{\infty} \left\{ \frac{1}{1+k} \left( 1 - \frac{2d_0}{l} \right)^{2k} \left[ \frac{21}{32} \alpha_k \left( \frac{2d_0}{l} \right)^{10} - \beta_k \left( \frac{2d_0}{l} \right)^4 \right] \right\} \quad (20)$$

The parameters  $K_{\text{AS}}$  and  $K_{\text{Aa}}$  can be calculated according to Equations (17) and (18). Parameters  $\alpha_k$  and  $\beta_k$  are defined as given in Equations (21) and (22):

$$\alpha_k = \left( \frac{-4,5-k}{k} \right)^2 \alpha_{k-1} \quad (21)$$

$$\beta_k = \left( \frac{-1,5-k}{k} \right)^2 \beta_{k-1} \quad (22)$$

where  $\alpha_0 = \beta_0 = 1$ .

In order to perform the HK and SF calculations, it is necessary to know the values for the adsorbent parameters  $\alpha_s, \chi_s, d_s, N_s$  as well as the adsorptive parameters  $\alpha_a, \chi_a, d_a$  and  $N_a$ . The results are very sensitive with regard to the choice of these constants. In Annex A, material parameters, taken from DIN 66135-4 [23], for the systems nitrogen/carbon and argon/zeolite.

## 9.5 Determination of micropore size distribution by non-local density functional theory

### 9.5.1 Background

Non-local density functional theory (NLDFT) and computer simulation methods, such as molecular dynamics and Monte Carlo simulation, have been developed into powerful methods for the description of the sorption and phase behaviour of inhomogeneous fluids confined to porous materials [24],[25],[26],[27],[28],[29],[30],[31],[32]. These methods accurately describe the structure of simple confined fluids, i.e. the oscillating density profiles near solid surfaces, or of fluids confined to simple geometries, such as slits, cylinders and spheres. They allow the calculation of equilibrium density profiles of a fluid, both adsorbed on surfaces and in pores, from which the adsorption/desorption isotherms, heats of adsorption and other thermodynamic quantities can then be derived. Pioneering studies on the application of the density functional theory (DFT) and molecular modeling by computer simulation in order to study the adsorption and phase behaviour of fluids in pores were performed by Evans and Tarazona [24]. Seaton, *et al.* [25] were the first to apply DFT for the calculation of the pore size distribution in both the meso- and micropore range. In this first attempt of applying DFT to pore size analysis, the so-called local version of DFT was used. It represents a significant improvement over the macroscopic, thermodynamic descriptions of pore filling, but is still inaccurate for narrow micropores. A significant improvement in accuracy was obtained with NLDFT, which was first reported for the pore size analysis of microporous carbons in 1993 by Lastoskie, *et al.* [26]. Since then, the NLDFT has been applied frequently for the pore size analysis of micro and mesoporous materials; see, for example, References [27], [28]. The NLDFT method is now commercially available for many adsorbent/adsorptive systems. Compared to the classical macroscopic thermodynamic models, the NLDFT methods describe behaviour of fluids confined in the pores on a molecular level. This application relates the molecular properties of gases to their adsorption properties in pores of different sizes. It follows that pore size characterization methods based on the NLDFT approach are applicable to the whole range of micro- and mesopores; see, for example, References [26], [28].

### 9.5.2 General approach of non-local density functional theory

Under experimental conditions, the adsorbed fluid in a pore is in equilibrium with a bulk gas phase, and accordingly, the conventional NLDFT treatment describes the system in terms of the grand canonical ensemble. The grand canonical potential function,  $\Omega[\rho(r)]$ , is given by Equation (23):

$$\Omega[\rho(r)] = F[\rho(r)] - \int dr \rho(r) [\mu - v_{\text{ext}}(r)] \quad (23)$$

where

- $\rho(r)$  is the equilibrium fluid density at a general 3D-space coordinate,  $r$ ;
- $F$  is the intrinsic Helmholtz free energy, which, in the absence of any external field, is expressed as a function,  $F[\rho(r)]$ , of the molecular density distribution,  $\rho(r)$ , of the gas at equilibrium;
- $v_{\text{ext}}(r)$  is the external potential imposed by the walls;
- $\mu$  is the chemical potential.

The external potential,  $v_{\text{ext}}(r)$ , depends on the assumed pore model.

For example, for the slit-shaped pore model, often used to describe carbon pores, this potential takes the form of Equation (24) to calculate the external potential,  $v_{\text{ext}}(z)$ :

$$v_{\text{ext}}(z) = \phi_{\text{sf}}(z) + \phi_{\text{sf}}(W - z) \quad (24)$$

where

- $\phi_{\text{sf}}(z)$  is the solid-fluid potential of interaction between the molecule and a pore wall;
- $W$  is the pore width;
- $z$  is the distance from the wall.

The solid-fluid potential usually accepted for porous carbons is the Steele potential [26], which describes interactions of a gas molecule with a single graphitic slab, as given in Equation (25):

$$\phi_{\text{sf}}(z) = 2\pi\varepsilon_{\text{sf}}\rho_{\text{s}}\sigma_{\text{sf}}\Delta \left[ \frac{2}{5} \left( \frac{\sigma_{\text{sf}}}{z} \right)^{10} - \left( \frac{\sigma_{\text{sf}}}{z} \right)^4 - \frac{\sigma_{\text{sf}}^4}{3\Delta(z + 0,61\Delta)^3} \right] \quad (25)$$

where

- $\varepsilon_{\text{sf}}$  is the well-depth parameter of the gas–wall interaction; noted as  $\varepsilon_{\text{sf}}/k_{\text{B}}$  in list of variables
- $\sigma_{\text{sf}}$  is the distance parameter of the gas–wall interaction;
- $\rho_{\text{s}}$  is the density of graphite;
- $\Delta$  is the distance between graphite layers.

Other pore-shaped models and their appropriate potentials, including cylindrical [33] and spherical [34] geometries, which are applicable to some mesoporous silica molecular sieves (e.g. MCM-41, SBA-16), are also considered.

The intrinsic free energy,  $F$ , is composed of three components:

- a) ideal gas free energy,  $F_{\text{id}}$ , which can be expressed by an exact expression [24];
- b) excess free energy,  $F_{\text{ex}}$ , which takes into account two types of interparticle interactions:
  - $F_{\text{att}}$ , the free energy arising from the attractive interactions;
  - $F_{\text{HS}}$ , the repulsive forces between molecules, described as a reference system of hard spheres.

The three components of the free energy,  $F$ , all being functions of the fluid density distribution, can be expressed as given in Equation (26):

$$\rho(\mathbf{r}): F[\rho(\mathbf{r})] = F_{\text{id}}[\rho(\mathbf{r})] + F_{\text{att}}[\rho(\mathbf{r})] + F_{\text{HS}}[\rho(\mathbf{r})] \quad (26)$$

The attractive interactions term,  $F_{\text{att}}$ , is calculated from Equation (27):

$$F_{\text{att}} = \frac{1}{2} \iint d\mathbf{r} d\mathbf{r}' \rho(\mathbf{r}) \rho(\mathbf{r}') \phi_{\text{att}}(|\mathbf{r} - \mathbf{r}'|) \quad (27)$$

where  $\phi_{\text{att}}$  is the attractive potential, modelled by the Weeks-Chandler-Anderson (WCA) approach [25], as given in Equation (28) for  $r_{\text{sc}} < r_{\text{m}}$  and in Equation (29) for  $r_{\text{m}} < r_{\text{sc}}$ :

$$\phi_{\text{att}}(r_{\text{sc}}) = -\varepsilon_{\text{ff}} \quad (28)$$

$$\phi_{\text{att}}(r_{\text{sc}}) = 4\varepsilon_{\text{ff}} \left[ \left( \sigma_{\text{ff}}/r_{\text{sc}} \right)^{12} - \left( \sigma_{\text{ff}}/r_{\text{sc}} \right)^6 \right] \quad (29)$$

where

$r_{\text{sc}}$  is the distance (scalar value) between the molecules;

$r_{\text{m}}$  is the minimum of the potential;

$\varepsilon_{\text{ff}}$  is the well-depth of the Lennard-Jones fluid-fluid interaction potential;

$\sigma_{\text{ff}}$  is the distance parameters of the Lennard-Jones fluid-fluid interaction potential.

The WCA approach has been proven to give good results when compared to Monte Carlo simulations [28].

In order to take into account repulsive forces, several functions for inhomogeneous hard-sphere fluids have been developed. Among them are the weighted-density approximation [29], the fundamental measure theory [30], [31], and the smoothed-density approximation [23]. The smoothed-density approximation, which was put forward by Tarazona, *et al.* [24], is used in almost all NLDFT versions currently applied for pore size characterization. In this approach, the free energy,  $F_{\text{HS}}[\rho(\mathbf{r})]$ , of the hard-sphere system is calculated for the smoothed density,  $\bar{\rho}(\mathbf{r})$ , as given in Equation (30):

$$F_{\text{HS}}[\rho(\mathbf{r})] = \int d\mathbf{r} \rho(\mathbf{r}) f_{\text{HS}}[\bar{\rho}(\mathbf{r}); d_{\text{HS}}] \quad (30)$$

where

$d_{\text{HS}}$  is the hard-sphere diameter;

$f_{\text{HS}}[\bar{\rho}(\mathbf{r}); d_{\text{HS}}]$  is the excess free energy per molecule, which can be calculated from the Carnahan-Starling equation of state for hard sphere fluid [24], [28].

Smoothed density,  $\bar{\rho}(\mathbf{r})$ , is obtained using the weighting function proposed by Tarazona [24].

The molecular-density distribution,  $\rho(\mathbf{r})$ , is the key description of the equilibrium fluid distribution in a given model pore. Based on the equilibrium condition, the density function,  $\rho(\mathbf{r})$ , is determined by minimizing the corresponding grand potential,  $\Omega[\rho(\mathbf{r})]$ . The minimum for  $\Omega$  is found by using the Euler-Lagrange equation [24] or the method of indeterminate Lagrange multipliers [32]. The actual numerical evaluation of  $\rho(\mathbf{r})$  is obtained in an iterative numerical process. Once  $\rho(\mathbf{r})$  is known, other thermodynamic properties, such as the adsorption isotherm, heat of adsorption, free energies, phase transitions, etc., can be calculated.

### 9.5.3 Application of pore size analysis — NLDFT kernel and integral adsorption equation

To apply the theory in practice for the calculation of the pore size distributions from the experimental adsorption isotherms, it is necessary to calculate theoretical, model isotherms using methods of statistical mechanics. In essence, these isotherms are calculated by integration of the equilibrium density profiles,  $\rho(r)$ , of the fluid in the model pores. A set of isotherms calculated for a set of pore sizes in a given range for a given adsorbate constitutes the model database. Such a set of isotherms, called a kernel, can be regarded as a theoretical reference for a given adsorption system and, as such, can be used to calculate pore size distributions from adsorption isotherms measured for the corresponding systems.

It is important to realize that the numerical values of a given kernel depend on a number of factors, such as the assumed geometrical pore model, values of the gas-gas and gas-solid interaction parameters and other model assumptions. It is a general practice to adjust the interaction parameters (fluid-fluid and fluid-solid) in such a way that the model correctly reproduces the fluid bulk properties (e.g. bulk liquid-gas equilibrium densities and pressures, liquid-gas interfacial tensions). Correct prediction of the surface tension is a necessary condition for any model used for the quantitative description of the capillary condensation/desorption transition in pores. The parameters of the solid-fluid potential are chosen to fit the standard adsorption isotherms on well defined, non-porous adsorbents [28].

A number of adsorption models have been studied and the parameters evaluated for gas adsorption on various materials published in the literature. For instance, gas-gas and gas-solid interaction parameters for the systems nitrogen/carbon, carbon dioxide/carbon and argon/carbon can be found in References [26], [28], [35], [36]. Appropriate interaction parameters for the systems nitrogen/silica and argon/silica are given in References [28] and [37]. References to the values of parameters used for the DFT analysis of several adsorption systems are listed in Tables B.1 and B.2.

The calculation of the pore size distribution is based on a solution of the integral adsorption equation (IAE) [4], which correlates the kernel of theoretical adsorption/desorption isotherms with the experimental sorption isotherm.  $N(p/p_0)$ , the adsorbed volume data from the experimental sorption isotherm, can be calculated from the IAE equation, as given in Equation (31):

$$N(p/p_0) = \int_{W_{\min.}}^{W_{\max.}} N(p/p_0, W) f(W) dW \quad (31)$$

where

$W$  is the pore width (distance between opposite walls of slit; diameter of cylindrical and spherical pores);

$N(p/p_0, W)$  is the kernel of the theoretical isotherms in pores of different widths;

$f(W)$  is the pore size distribution function.

The IAE equation reflects the assumption that the total isotherm consists of a number of individual "single-pore" isotherms multiplied by their relative distribution,  $f(W)$ , over a range of pore sizes. The set of  $N(p/p_0, W)$  isotherms (kernel) for a given system (adsorptive/adsorbent) can be obtained by either density functional theory or by Monte-Carlo computer simulation. Pore size distribution is then derived by numerically solving the IAE equation. In general, the solution of the IAE represents an ill-posed problem, which requires some degree of regularization. The existing regularization algorithms [38], [39], [40] allow meaningful and stable solutions of this equation to be obtained. In order to confirm the validity of the calculation, compare the calculated NLDFT (fitting) isotherm with the experimental sorption isotherm.



## 10 Test report

A summary of the measurement conditions and constants used in the calculation should be provided with each result, as follows:

- a) laboratory, operator, date;
- b) sample identification, e.g. chemical composition, purity, particle size distribution, method of sampling, sample division;
- c) sample source;
- d) mass,  $m_s$ , of outgassed sample, expressed in grams;
- e) experimental method and instrument used;
- f) sample pretreatment;
- g) outgassing conditions: temperature and evacuation pressure;
- h) calibration constants;
- i) model/method used for pore size and surface area analysis;
- j) materials parameters for adsorptive and adsorbent when SF and HK method are applied;
- k) description of kernel (e.g. adsorptive/adsorbent pair, assumed pore geometry, adsorption/desorption branch) when the NLDFT method is applied;
- l) micropore volume, expressed in cubic centimetres per gram;
- m) total pore volume, expressed in cubic centimetres per gram;
- n) specific surface area, expressed in square metres per gram;
- o) plots and tables of cumulative pore volume, and pore volume distribution (for HK, SF and NLDFT methods).

## Annex A (informative)

### Horvath-Kawazoe and Saito-Foley methods

#### A.1 Examples for material constants, adsorbent and adsorptive parameters

NOTE See DIN 66135-4.

Examples for adsorptive and adsorbent model parameters for application in Horvath-Kawazoe and Saito-Foley are given in Tables A.1 and A.2. The constants were taken from the original papers of Horvath-Kawazoe<sup>[19], [20]</sup> and Saito-Foley<sup>[21], [22]</sup>. Please note that non-uniform values of the parameters given in the Tables A.1 and A.2 can be found in the literature. Hence, in order to present significant results, it is crucial that the adsorbent and adsorptive parameters employed in the SF and HK calculations be stated in the analysis report.

**Table A.1 — Adsorbent parameters**

Physical quantity	Unit	Symbol	Carbon <sup>a</sup>	Zeolite <sup>b</sup>
Polarizability	$10^{-24} \text{ cm}^3$	$\alpha_{(s^*)}$	1,02	2,50
Magnetic susceptibility	$10^{-29} \text{ cm}^3$	$\chi_s$	13,5	1,30
Surface density (atoms per square metre of pore wall)	$10^{19} \text{ m}^{-2}$	$N_s$	3,84	1,31
Diameter	nanometre	$d_s$	0,34	0,28
<sup>a</sup> See References [19] and [20].				
<sup>b</sup> See References [21] and [22].				

**Table A.2 — Adsorptive parameters**

Physical quantity	Unit	Symbol	Nitrogen <sup>a</sup>	Argon <sup>b</sup>
Polarizability	$10^{-24} \text{ cm}^3$	$\alpha_a$	1,46	1,63
Magnetic susceptibility	$10^{-29} \text{ cm}^3$	$\chi_a$	2,00	3,25
Surface density (atoms per square metre of monolayer)	$10^{18} \text{ m}^{-2}$	$N_a$	6,70	8,52
Diameter	nanometre	$d_s$	0,30	0,34
<sup>a</sup> See References [19] and [20].				
<sup>b</sup> See References [21] and [22].				

The values given in Table A.3 are calculated using the materials constants for adsorptive and adsorbents given in Tables A.1 and A.2.

**Table A.3 — Relation between the pore diameter and the relative pressure where micropore filling of nitrogen occurs at 77,35 K in a carbon slit pore according to the Horvath-Kawazoe approach**

$d_p$ nm	0,4	0,5	0,6	0,7	0,8	1,0	1,2	1,4	1,7	2,0
$p/p_0$	$1,8 \times 10^{-7}$	$1,2 \times 10^{-5}$	$1,7 \times 10^{-4}$	$9,6 \times 10^{-4}$	$3,2 \times 10^{-3}$	$1,4 \times 10^{-2}$	$3,5 \times 10^{-2}$	$6,3 \times 10^{-2}$	$1,1 \times 10^{-1}$	$1,6 \times 10^{-1}$

The values given in Table A.4 are calculated using the materials constants given in Tables A.1 and A.2.

**Table A.4 — Relation between the pore diameter and the relative pressure where micropore filling of argon occurs at 87,27 K in a cylindrical zeolite pore according to the Saito-Foley approach**

$d_p$ nm	0,4	0,5	0,6	0,7	0,8	1,0	1,2	1,4	1,7	2,0
$p/p_0$	$5,7 \times 10^{-7}$	$9,8 \times 10^{-6}$	$1,4 \times 10^{-4}$	$8,7 \times 10^{-4}$	$3,1 \times 10^{-3}$	$1,5 \times 10^{-2}$	$3,9 \times 10^{-2}$	$7,2 \times 10^{-2}$	$1,3 \times 10^{-1}$	$1,9 \times 10^{-1}$

## A.2 Example of the application of the Saito-Foley micropore analysis

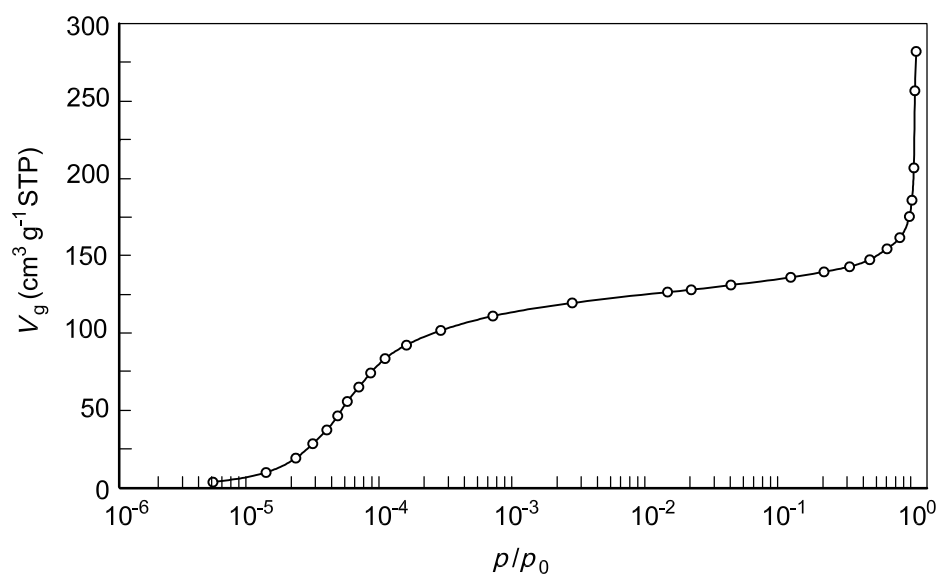
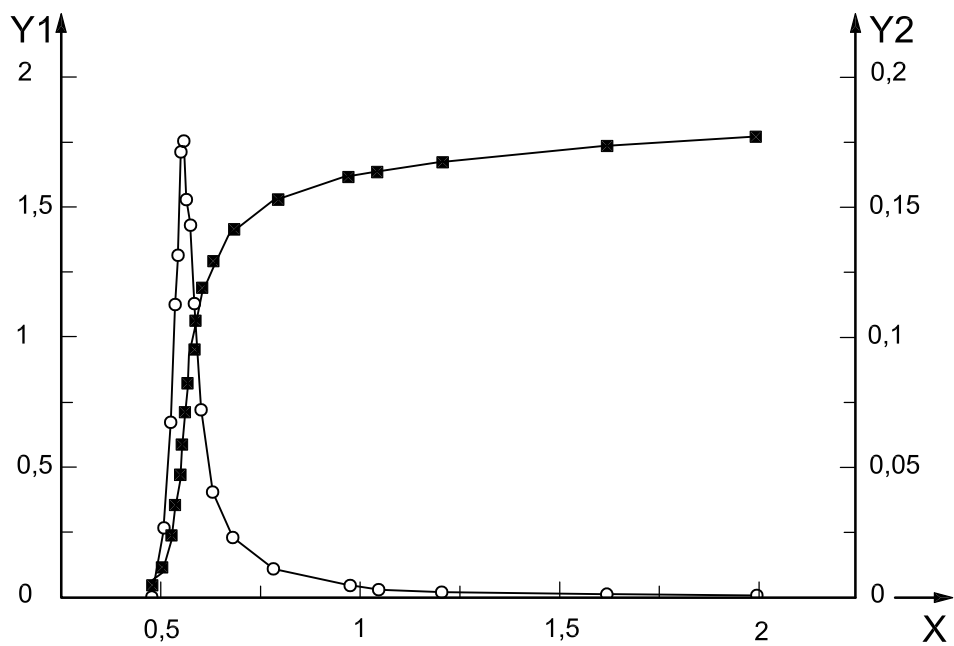


**Figure A.1 — Experimental argon adsorption isotherm on a type A zeolite at 87,3 K**



**Key**

- X pore diameter, expressed in nanometres
- Y1 differential pore volume, expressed in cubic centimetres per gram per nanometre
- Y2 cumulative pore volume, expressed in cubic centimetres per gram
- cumulative pore volume
- differential pore volume

**Figure A.2 — Saito-Foley pore size analysis of type A zeolite**

The values plotted in Figure A.2 are obtained from the argon sorption isotherm shown in Figure A.1. The adsorptive and adsorbent parameters used in the calculation correspond to the values given in Tables A.1 and A.2.

## Annex B (informative)

### NLDFT method

#### B.1 Examples of adsorptive and adsorptive-adsorbent interaction parameters for use in NLDFT calculations

**Table B.1 — Parameters of the adsorptive-adsorptive intermolecular potentials for NLDFT calculations**

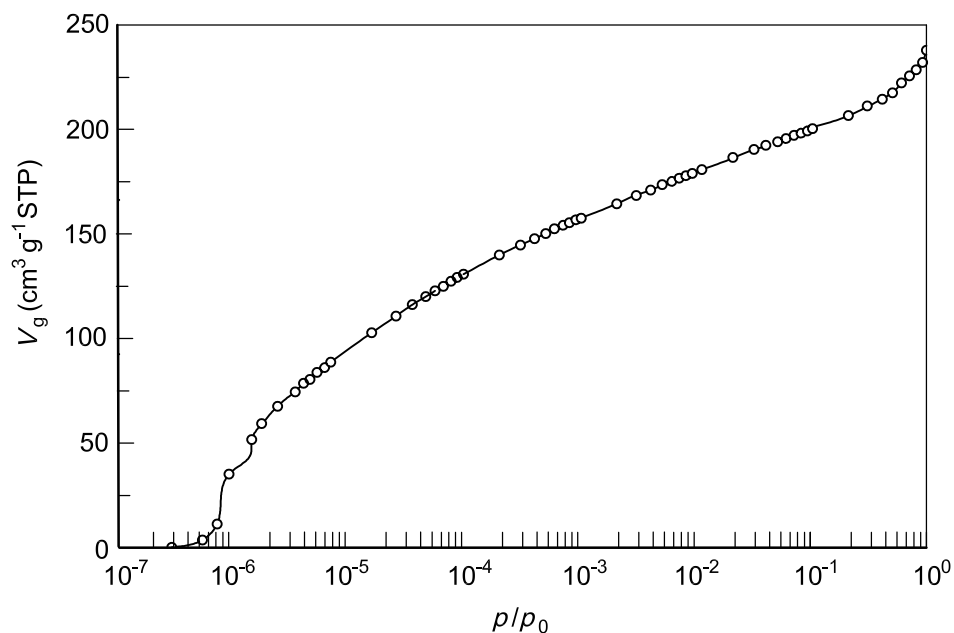
Gas	$\varepsilon_{ff}/k_B$ K	$\sigma_{ff}$ nm	$\delta_{HS}$ nm
Nitrogen <sup>a</sup>	94,45	0,357 5	0,357 5
Argon <sup>b</sup>	118,05	0,330 5	0,338 0
Carbon dioxide <sup>a</sup>	253,9	0,345 4	0,349 5
<sup>a</sup> See References [28] and [36]. <sup>b</sup> See Reference [37].			

**Table B.2 — Parameters for adsorptive-adsorbent intermolecular potentials for NLDFT calculations**

Gas-solid	$\varepsilon_{sf}/k_B$ K	$\sigma_{sf}$ nm	$N_s$
Nitrogen-carbon <sup>b</sup>	53,22	0,349 4	Carbon <sup>a</sup> : $N_s = 0,038\ 19\ \text{nm}^{-2}$
Carbon dioxide-carbon <sup>b</sup>	81,5	0,343 0	—
Nitrogen-silica <sup>c</sup>	147,3	0,317 0	Silica <sup>a</sup> : $N_s = 0,015\ 3\ \text{nm}^{-2}$
Argon-silica <sup>d</sup>	171,24	0,300 0	—
<sup>a</sup> See Reference [28]. <sup>b</sup> See References [28] and [36]. <sup>c</sup> See References [28] and [37]. <sup>d</sup> See Reference [37].			

## B.2 Example of the application of NLDFT micropore analysis

The plot in Figure B.1 was obtained by assuming a slit-pore model and using the adsorptive/adsorbent parameters as given in Tables B.1 and B.2 [36].

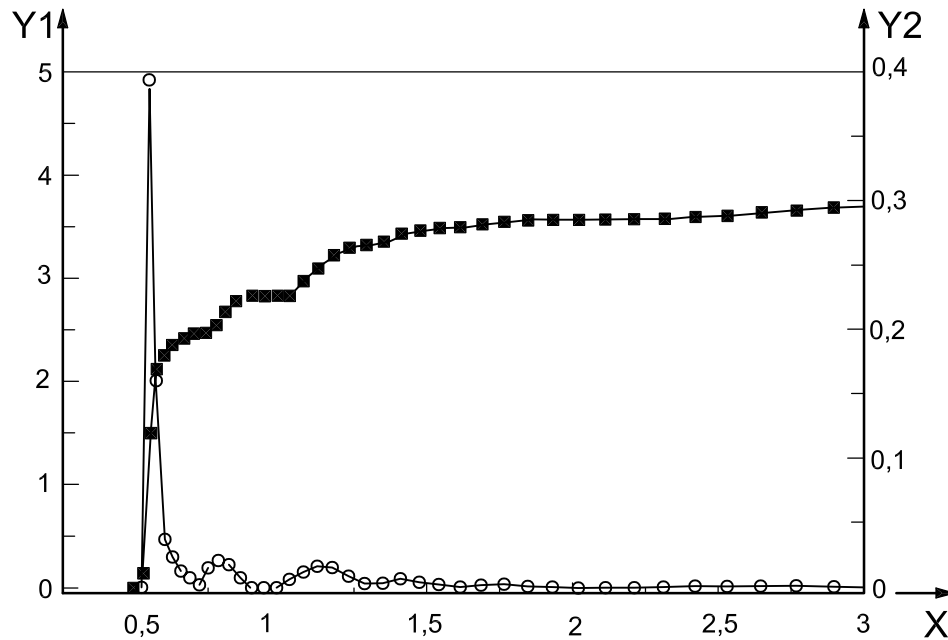


### Key

- nitrogen (77,3 K) on activated carbon fibre
- NLDFT fit

**Figure B.1 — Experimental nitrogen adsorption isotherm and NLDFT fit on activated carbon fibre (ACF) at 77,3 K**

The calculations for Figure B.2 were performed based on a slit-pore model and using the adsorptive and adsorbent interaction parameters given in Tables B.1 and B.2<sup>[34]</sup>.



#### Key

- X pore diameter, expressed in nanometres
- Y1 differential pore volume, expressed in cubic centimetres per gram per nanometre
- Y2 cumulative pore volume, expressed in cubic centimetres per gram
- cumulative pore volume
- differential pore volume

**Figure B.2 — NLDFT pore size analysis of activated carbon fibre obtained from the nitrogen adsorption isotherm shown in Figure B.1**

## Bibliography

- [1] GREGG, S.J., SING, K.S.W. *Adsorption, Surface Area and Porosity*. 2nd ed., Academic Press, London 1982
- [2] MIKHAIL, R.SH. AND ROBENS, E. *Microstructure and Thermal Analysis of Solid Surfaces*. Wiley, Chichester 1983
- [3] KANEKO, K. *Journal of Membrane Science*, **96** (1994), 59
- [4] ROSS, S., OLIVIER, J.P. *On Physical Adsorption*. Wiley and Sons, New York (1964)
- [5] CONNER, W.C. In: Fraissard, J. (Ed.), *Physical Adsorption: Experiment, Theory and Applications*. Kluwer, Dordrecht 1997, S. 33-63
- [6] LOWELL, S., SHIELDS, J.E., THOMAS, M.A. AND THOMMES M. *Characterization of Porous Solids and Powders: Surface Area, Pore Size and Density*. Kluwer, Dordrecht 2004
- [7] ROUQUEROL, F., ROUQUEROL, J., SING, K.S.W. *Adsorption by Powders and Porous Solids*. Academic Press, San Diego 1999
- [8] EVERETT, D.H. AND POWL, J.C. *J. Chem. Soc. Faraday Trans. I*, **72** (1976) 619
- [9] DUBININ, M.M. *Quart. Rev. Chem. Soc.*, **9** (1955), 101
- [10] DUBININ, M.M. In: *Progress in Surface and Membrane Science*, 9 (D.A. Cadenhead ed.), Academic Press 1975
- [11] DUBININ, M.M. *Chem. Rev.*, **60** (1969) 235
- [12] STOECKLI, H.F. *J. Colloid Interface Sci.*, **59** (1977), 1, 185
- [13] DUBININ, M.M., STOECKLI, H.F. *J. Colloid Interface Sci.*, **75** (1980), 1, 34
- [14] POLANYI, M. *Verh. dtsh. physik. Ges.*, **16** (1914), 1012
- [15] LIPPENS, B.C., LINSEN, B.G., DEBOER, J.H. *J. Catalysis*, **3** (1964), 32
- [16] LIPPENS, B.C., DEBOER, J.H. *J. Catalysis*, **4** (1965), 319
- [17] DEBOER, J.H., LINSEN, B.G., OSINGA, TH.J. *J. Catalysis*, **4** (1965), 643
- [18] SING, K.S.W. In: Everett, D.H., Ottewill, R.H. (eds.), *Surface Area Determination*. Butterworths, London 1970, 25
- [19] HORVATH, G. AND KAWAZOE, K. *J. Chem Eng. Japan*, **16** (1983), 470
- [20] HORVATH, G. Energetic interactions in phase and molecular level pore characterization in nano-range, *Colloids & Surfaces A: Physicochemical and Engineering Aspects*, **141** (1998), 295 – 304
- [21] SAITO, A., FOLEY, C. *AIChE Journal*, **37** (1991), 429
- [22] SAITO, A., FOLEY, C. *Microporous Materials*, **3** (1995), 531
- [23] DIN 66135-4, *Partikelmesstechnik — Mikroporenanalyse mittels Gasadsorption — Teil 4: Bestimmung der Porenverteilung nach Horvath-Kawazoe und Saito-Foley*



- [24] TARAZONA, P. *Physical Review*, **31**, 2672 (1985); EVANS, R., TARAZONA, P. *Phys. Rev. A*, **31** (1985), 2672; TARAZONA, P., EVANS, R. *Mol Phys.*, **52** (1984), 847
- [25] SEATON, N.A., WALTON, J.R.B., QUIRKE, N. *Carbon*, **27** (1989), 853
- [26] LASTOSKIE, C.M., GUBBINS, K., QUIRKE, N. *J. Phys. Chem.*, **97** (1993), 4786
- [27] OLIVIER, J.P. *J. Porous Mat.*, **2** (1995), 9
- [28] RAVIKOVITCH, P., VISHNYAKOV, A., NEIMARK, A.V. *Phys. Rev. E* **64** (2001), 011602
- [29] CURTIN, W.A., ASHCROFT, N.W. *Phys. Rev. A* **32** (1985), 2909
- [30] KIERLIK, E., ROSINBERG, M.L. *Phys. Rev. A* **42** (1990), 3382
- [31] ROSENFELD Y. *Phys. Rev. Lett.*, **63** (1989), 980
- [32] NEIMARK, A.V. *Langmuir*, **11** (1995), 4183
- [33] RAVIKOVITCH, P.I., DOMHNAILL, S.C., NEIMARK, A.V., SCHUETH, F., UNGER, K.K. *Langmuir*, **11** (1995), 4765
- [34] RAVIKOVITCH, P.I. AND NEIMARK, A.V. *Langmuir*, 2002, **18**, 1550
- [35] SWEATMAN, M.B. AND QUIRKE, N. *Langmuir*, **17** (2001), 5011
- [36] RAVIKOVITCH, P.I., VISHNYAKOV, A., RUSSO, R. AND NEIMARK, A.V. *Langmuir*, **16** (2000), 2311
- [37] NEIMARK, A.V., RAVIKOVITCH, P.I. *Microporous and Mesoporous Material*, 44-45 (2001), 697
- [38] LAWSON, C.L., HANSON, R.J. *Solving least squares problems SIAM*, Philadelphia, 1995
- [39] PROVENCHER, S.W. *Computer Phys. Commun.*, **27** (1982), 213
- [40] WAHBA, G., *SIAM J. Numer. Anal.*, **14** (1977), 651
- [41] IUPAC Recommendations 1984, SING, K.S.W., EVERETT, D.H., HAUL, R.A.W., MOSCOU, L., PIEROTTI, R.A., ROUQUÉROL, J., SIEMIENIEWSKA, T. "Reporting Physisorption Data for Gas/Solid Systems with Special Reference to the Determination of Surface Area and Porosity", *Pure & Appl. Chem.*, **57** (1985), 4, 603-619
- [42] IUPAC Recommendations 1994, ROUQUÉROL, J., AVNIR, D., FAIRBRIDGE, C.W., EVERETT, D.H., HAYNES, J.H., PERNICONE, N., RAMSAY, J.D.F., SING, K.S.W., UNGER, K.K. "Recommendations for the Characterization of Porous Solids", *Pure & Appl. Chem.*, **66** (1994), 8, 1739-1785
- [43] ISO 31-0, *Quantities and units — Part 0: General principles*

---

---

**ICS 19.120**

Price based on 27 pages